

# A natural frequency sensitivity-based stabilization in spectral stochastic finite element method for frequency response analysis

Gil-Yong Lee<sup>1</sup>, Seung-Seop Jin<sup>2</sup> and Yong-Hwa Park<sup>\*1</sup>

<sup>1</sup>Department of Mechanical Engineering, KAIST, 291 Daehak-ro Yuseong-gu Daejeon 34141, Republic of Korea

<sup>2</sup>Sustainable Infrastructure Research Center, Korea Institute of Civil Engineering and Building Technology (KICT), Goyang-Si 10223, Republic of Korea

(Received December 22, 2019, Revised February 24, 2020, Accepted February 25, 2020)

**Abstract.** In applying the spectral stochastic finite element methods to the frequency response analysis, the conventional methods are known to give unstable and inaccurate results near the natural frequencies. To address this issue, a new sensitivity based stabilized formulation for stochastic frequency response analysis is proposed in this paper. The main difference over the conventional spectral methods is that the polynomials of random variables are applied to both numerator and denominator in approximating the harmonic response solution. In order to reflect the resonance behavior of the structure, the denominator polynomials is constructed by utilizing the natural frequency sensitivity and the random mode superposition. The numerator is approximated by applying a polynomial chaos expansion, and its coefficients are obtained through the Galerkin or the spectral projection method. Through various numerical studies, it is seen that the proposed method improves accuracy, especially in the vicinities of structural natural frequencies compared to conventional spectral methods.

**Keywords:** uncertainty quantification; spectral stochastic finite element method; frequency response; natural frequency sensitivity

## 1. Introduction

In structural mechanics, the finite element method (FEM) has been widely used in many engineering problems and applications. Usually, computational models are considered to be deterministic that one particular set of parameters is used. However, most physical systems, in reality, are subject to uncertainties about the input parameters such as material properties, loading, and geometry conditions. In this context, uncertainty modeling and propagation (uncertainty analysis) are necessary to consider response variability for decision-making.

The stochastic finite element method (SFEM) is an extension of deterministic FEM to study response variability under uncertain parametric input conditions (Stefanou 2009). In the probabilistic framework, the uncertain parameters are treated as a combination of random variables and fields so that the governing equations become stochastic. To obtain solution characteristics, several methods have been proposed such as Monte Carlo simulation (MCS), perturbation, Neumann expansion method, and spectral stochastic method. MCS (Papadrakakis and Papadopoulos 1996, Hurtado and Barbat 1998) is a sampling-based technique and is considered the most robust method for uncertainty quantification. Although MCS is easily applied regardless of the dimensionality of parameters and non-linearity of models, a large number of samples should be drawn independently to obtain sufficient

accuracy with reasonable precision. As a result, the computational cost becomes prohibitive. The perturbation-based method (Kleiber and Hien 1992) is a low-order Taylor expansion based technique that approximates the solution near the mean value of parameters, while the Neumann expansion method (Yamazaki, Shinozuka *et al.* 1988) approximates the inverse matrix as a convergent series. Although these two methods are computationally efficient, the obtained solutions are inaccurate under large parameter variability.

The spectral stochastic finite element method (SSFEM) (Ghanem and Spanos 2003) approximates the solution using polynomial chaos expansion (PCE), which is constructed depending on the probability distribution of the uncertain parameters (Xiu and Karniadakis 2002). Since SSFEM can be applied to various levels of uncertainty, it has gained considerable attention in uncertainty analysis. The coefficients of the PCE basis are unknown and can be obtained either via an intrusive approach (a non-sampling method such as Galerkin projection (Ghanem and Spanos 2003, Galal, El-Tahan *et al.* 2008)) or a non-intrusive approach (a sampling method such as the spectral projection method or regression method (Berveiller, Sudret *et al.* 2006)). One of the disadvantages is that the number of required PCE basis increases exponentially as the number of random variable increases. Due to this problem, conventional PCE methods are only applicable up to moderate dimensionality of the parameters. There are several methods to address the dimensionality problem for both intrusive (Nouy 2007) and non-intrusive methods (Xiu and Hesthaven 2005, Blatman and Sudret 2011).

Despite the advantages of SSFEM, many studies have been mainly applied to linear static analysis. Recently, there

\*Corresponding author, Ph.D., Professor  
E-mail: [yhpark@kaist.ac.kr](mailto:yhpark@kaist.ac.kr)

have been several attempts to incorporate SSFEM into a stochastic frequency response analysis (Adhikari 2011, Jacquelin, Adhikari *et al.* 2014, Sinou and Jacquelin 2015, Sepahvand 2016). Jacquelin, Adhikari *et al.* reported that, around the natural frequencies, the frequency responses become very inaccurate and show spurious oscillations (Jacquelin, Adhikari *et al.* 2014). The effect of damping was investigated in (Adhikari and Pascual 2016), and they reported that if the modal damping ratio is larger than 10%, spurious oscillations near natural frequencies might be suppressed due to the nature of damping. However, when the damping becomes small (about 1%) the situation changes dramatically and erroneous results will be obtained. To alleviate this problem, Aitken's transformation and its generalization approach were applied to estimate the first two statistical moments of the frequency response (Jacquelin, Adhikari *et al.* 2015). Also, they showed that the convergence rate of two statistical moments can be improved by changing the PCE basis (Jacquelin, Adhikari *et al.* 2016). A multi-element PCE method was proposed for modeling frequency responses in a single degree of freedom (SDOF) system (Pagnacco, Sarrouy *et al.* 2017). Since the multi-element PCE method may increase the number of random variables, a Proper Generalized Decomposition (PGD) method was utilized to reduce computational costs (Chevreuil and Nouy 2012). A PCE-based Padé approximation (Jacquelin, Dessombz *et al.* 2017) was used to compute the response and it is shown that the denominator plays a key role in the stochastic frequency response.

Although many types of studies have been carried out previously, it is difficult to apply the PCE framework to the stochastic frequency response analysis, and a simple algorithm is still needed. Since the shift of natural frequencies due to random parameter variation results in a highly non-smooth behavior, conventional PCE methods cannot capture actual responses near the natural frequencies. To overcome this phenomenon, we propose a sensitivity-based stabilization for SSFEM by combining conventional PCE and natural frequency sensitivity. The proposed method utilizes the sensitivity of the natural frequency that provides prior information about the solution characteristics. The combined solution form is a rational function, and it can be easily applied to existing spectral stochastic algorithms.

The rest of this paper is organized as follows. In Section 2, we present the background of the stochastic frequency response analysis. Section 3 describes the proposed method of combining the PCE and sensitivity. In Section 4, the proposed method is verified through various numerical studies. Finally, we provide concluding remarks in Section 5.

## 2. Formulation of spectral stochastic frequency response

### 2.1 Modeling of spatial random field

Prior to performing the stochastic finite element analysis, input uncertainties should be parameterized using the random variables that follow an appropriate probability

distribution. If the uncertainty is modeled as a spatially distributed random field, it can be represented by spectral decomposition utilizing a truncated Karhunen-Loève (KL) expansion as (Ghanem and Spanos 2003, Hussein, El-Tawil *et al.* 2008)

$$a(\mathbf{x}, \boldsymbol{\xi}) = a_0(\mathbf{x}) + \sum_{i=1}^K \sqrt{\gamma_i} \xi_i g_i(\mathbf{x}) \quad (1)$$

where  $a(\mathbf{x}, \boldsymbol{\xi})$  is the random field,  $\mathbf{x}$ ,  $\boldsymbol{\xi}$  are the position vector defined over the spatial domain and the random variables on a probability space;  $a_0(\mathbf{x})$ ,  $K$  are mean of the random field and the total number of truncated random variables.  $\gamma_i$  and  $g_i$  are  $i$ th eigenvalue and eigenvector that satisfy the following Fredholm integral equation of the second kind

$$\int C_a(\mathbf{x}_1, \mathbf{x}_2) g_i(\mathbf{x}_2) d\mathbf{x}_2 = \gamma_i g_i(\mathbf{x}_1) \quad (2)$$

where  $C_a(\mathbf{x}_1, \mathbf{x}_2)$  is a covariance function of the given random field  $a(\mathbf{x}, \boldsymbol{\xi})$  and  $\mathbf{x}_1, \mathbf{x}_2$  are arbitrary position vector in the domain. If the random field follows a Gaussian distribution, the corresponding  $\boldsymbol{\xi}$  is uncorrelated standard normal random variables. For a non-Gaussian random field, it can be represented by applying the polynomial chaos expansion (Sakamoto and Ghanem 2002).

In solving the integral equation in Eq. (2), an analytical solution does not always exist in the case of arbitrary geometry and covariance function. Therefore, the finite element method (FEM), one of the numerical approaches is adopted in this paper. Based on the discretized geometry, applying the Galerkin projection to Eq. (2) yields the following symmetric eigenvalue problem

$$\begin{aligned} \mathbf{C}_a \mathbf{g}_i &= \gamma_i \mathbf{B} \mathbf{g}_i \\ \mathbf{C}_a &= \int \int \mathbf{N}^T(\mathbf{x}_1) C_a(\mathbf{x}_1, \mathbf{x}_2) \mathbf{N}(\mathbf{x}_2) d\mathbf{x}_2 d\mathbf{x}_1 \\ \mathbf{B} &= \int \mathbf{N}^T(\mathbf{x}_1) \mathbf{N}(\mathbf{x}_1) d\mathbf{x}_1 \end{aligned} \quad (3)$$

where  $\mathbf{N}$ ,  $\mathbf{g}_i$  are the shape function matrix and the  $i$ th discretized eigenvector, respectively. Referring to Eq. (3), one problem in constructing the discretized covariance matrix  $\mathbf{C}_a$  is that it contains a double integral, which may require a high computational cost. To address this issue, the covariance matrix is approximated with the spatial shape functions as follows (Kundu, Adhikari *et al.* 2014):

$$\mathbf{C}_a(\mathbf{x}_1, \mathbf{x}_2) \approx \mathbf{N}(\mathbf{x}_1) \tilde{\mathbf{C}}_a \mathbf{N}^T(\mathbf{x}_2) \quad (4)$$

where  $\tilde{\mathbf{C}}_a$  is the discrete covariance matrix, and each component is the covariance function value between two nodes. By substituting Eq. (4) into Eq. (3), the covariance matrix  $\mathbf{C}_a$  is expressed as

$$\begin{aligned} \mathbf{C}_a &\approx \int \mathbf{N}^T(\mathbf{x}_1) \mathbf{N}(\mathbf{x}_1) d\mathbf{x}_1 \tilde{\mathbf{C}}_a \int \mathbf{N}^T(\mathbf{x}_2) \mathbf{N}(\mathbf{x}_2) d\mathbf{x}_2 \\ &= \mathbf{B} \tilde{\mathbf{C}}_a \mathbf{B} \end{aligned} \quad (5)$$

Since Eq. (5) only involves matrix multiplication, the numerical efficiency of constructing the system matrix can be effectively improved.

### 2.2 Stochastic structural dynamic problem in the frequency domain

In this study, a linear stochastic partial differential equation for an elastodynamic system is considered. The

governing equation on a domain  $\Omega$  is given by

$$\begin{aligned} \operatorname{div}(\sigma(u)) + b &= \rho \ddot{u} & \text{on } \Omega \\ u &= u_0 & \text{on } \Gamma_D \\ \sigma(u) \cdot n &= s & \text{on } \Gamma_N \end{aligned} \quad (6)$$

where  $\sigma(u)$ ,  $u_0$ ,  $s$ ,  $b$ , and  $\rho$  are the stress tensor, prescribed displacement, surface traction, body force, and density, respectively;  $\Gamma_D$  and  $\Gamma_N$  are Dirichlet and Neumann boundaries that satisfy  $\Gamma_D \cap \Gamma_N = \emptyset$  and  $\Gamma_D \cup \Gamma_N = \partial\Omega$ .

Based on the parametric uncertainties  $\xi$ , the discretization of Eq. (6) using FEM is well established in the linear static analysis (Ghanem and Spanos 2003) and can be easily extended to a dynamic case. In the presence of the damping, the stochastic linear dynamic system equation is expressed as

$$\mathbf{M}(\xi)\ddot{\mathbf{u}}(t, \xi) + \mathbf{C}(\xi)\dot{\mathbf{u}}(t, \xi) + \mathbf{K}(\xi)\mathbf{u}(t, \xi) = \mathbf{f}(t, \xi) \quad (7)$$

where  $\mathbf{M}(\xi)$ ,  $\mathbf{C}(\xi)$ , and  $\mathbf{K}(\xi)$  denotes the mass, damping, and stiffness matrices;  $\ddot{\mathbf{u}}(t, \xi)$ ,  $\dot{\mathbf{u}}(t, \xi)$ ,  $\mathbf{u}(t, \xi)$ , and  $\mathbf{f}(t, \xi)$  are acceleration, velocity, displacement, and the force vector, respectively. To obtain the frequency response of Eq. (7), the displacement and force vectors are assumed to be harmonic as  $\mathbf{u}(t, \xi) = \mathbf{U}(\omega, \xi)e^{i\omega t}$ ,  $\mathbf{f}(t, \xi) = \mathbf{F}(\xi)e^{i\omega t}$ , where  $\omega$  is the excitation frequency. Substituting these relations into Eq. (7), following stochastic frequency response equation is obtained

$$[-\omega^2\mathbf{M}(\xi) + i\omega\mathbf{C}(\xi) + \mathbf{K}(\xi)]\mathbf{U}(\omega, \xi) = \mathbf{F}(\xi) \quad (8)$$

The left side of Eq. (8) can be rewritten to be composed of deterministic  $\mathbf{A}_0$  and stochastic parts  $\mathbf{A}_i$  as

$$\left[ \sum_{i=0}^M \mathbf{A}_i(\omega, \xi) \right] \mathbf{U}(\omega, \xi) = \mathbf{F}(\xi) \quad (9)$$

where  $M$  represents the total number of random variables in the dynamic system and each matrix can be expressed as

$$\begin{aligned} \mathbf{A}_0(\omega) &= (-\omega^2\mathbf{M}_0 + i\omega\mathbf{C}_0 + \mathbf{K}_0) \\ \mathbf{A}_i(\omega, \xi) &= -\omega^2\mathbf{M}_i(\xi) \quad \text{for } i = 1, 2, \dots, m_1 \\ \mathbf{A}_i(\omega, \xi) &= i\omega\mathbf{C}_i(\xi) \quad \text{for } i = m_1 + 1, \dots, m_1 + m_2 \\ \mathbf{A}_i(\omega, \xi) &= \mathbf{K}_i(\xi) \quad \text{for } i = m_1 + m_2 + 1, \dots \\ & m_1 + m_2 + m_3 = M \end{aligned} \quad (10)$$

where  $m_1$ ,  $m_2$ , and  $m_3$  denotes the number of random variables in the stiffness, damping, and mass matrix, respectively.

### 2.3 Overview of spectral stochastic methods

In the spectral stochastic methods, the solution of Eq. (9) with the number of random variables  $M$  is approximated in terms of a truncated polynomial chaos (PC) basis as

$$\mathbf{U}(\omega, \xi) = \sum_{j=1}^P \bar{\mathbf{U}}_j(\omega) \Psi_j(\xi) \quad (11)$$

where  $\Psi_j(\xi)$ ,  $\bar{\mathbf{U}}_j$  and  $P$  are the PC basis and coefficient vector, the number of PC basis, respectively. The PC basis

is a function of random variables with a dimension  $M$  and, depending on the given probability distribution, it can be constructed by applying the Wiener-Askey scheme (Xiu and Karniadakis 2002). If the  $i$ th random variable is assumed to follow the Gaussian distribution, the one-dimensional Hermite polynomials  $He_{n_i}(\xi_i)$  are given by

$$He_{n_i}(\xi_i) = (-1)^{n_i} \exp(\xi_i^2/2) \left[ \frac{d^{n_i}}{d\xi_i^{n_i}} \exp(-\xi_i^2/2) \right] \quad (12)$$

where  $n_i$  is the polynomial order of  $i$ th random variable. For the multi-dimensional case, the bases are constructed utilizing the tensor product of the one-dimensional polynomial bases. For example, the  $M$ -dimensional Hermite polynomials with order  $\mathbf{n} = \sum_{i=1}^M n_i$  are obtained as

$$He_{\mathbf{n}}(\xi) = \prod_{i=1}^M He_{n_i}(\xi_i) \quad (13)$$

One important characteristic of the PC basis is that it satisfies the following orthogonality for a given probability density function (PDF)

$$\begin{aligned} E[\Psi_j(\xi)\Psi_k(\xi)] &= \int \Psi_j(\xi)\Psi_k(\xi)f_\xi(\xi) d\xi \\ &= \delta_{jk}E[\Psi_j^2(\xi)] \end{aligned} \quad (14)$$

where  $E[\cdot]$ ,  $\delta_{jk}$ , and  $f_\xi(\xi)$  are the expectation operator, the Kronecker delta, and the joint probability density function, respectively. The number of basis  $P$  is determined by the number of random variables  $M$  and polynomial order  $p$  as follows:

$$P = \binom{M+p}{p} = \frac{(M+p)!}{M!p!} \quad (15)$$

where  $(\cdot)!$  denotes the factorial operator.

There are several ways to solve Eq. (9), through PC basis either intrusive or non-intrusive approach. The intrusive method requires modification of the existing deterministic solver (e.g., conventional FEM codes) that solves the enlarged equation at once (Ghanem and Spanos 2003), while the non-intrusive method utilizes an existing deterministic solver over random parameter space without any code modification (Smith 2013). This paper briefly overviews the Galerkin projection and spectral projection method, which are most widely used in SSFEM.

Galerkin projection is an intrusive method that projects the weighted residual on to the truncated PC space. Substituting Eq. (11) into (9) yields

$$\sum_{i=0}^M \mathbf{A}_i(\omega, \xi) \sum_{j=1}^P \bar{\mathbf{U}}_j \Psi_j(\xi) = \mathbf{F}(\xi) \quad (16)$$

Multiplying the PC basis  $\Psi_k(\xi)$  for  $k=1, \dots, P$ , and taking the expectation operator, the following equations are obtained

$$\sum_{i=0}^M \sum_{j=1}^P E[\Psi_k(\xi)\mathbf{A}_i(\omega, \xi)\Psi_j(\xi)] \bar{\mathbf{U}}_j = E[\Psi_k\mathbf{F}(\xi)] \quad (17)$$

These equations can be assembled into linear system equations of size  $NP$ , where  $N$  is total degrees of freedom (DOF), as follows:

$$\begin{bmatrix} \mathbf{A}_{11} & \mathbf{A}_{12} & \dots & \mathbf{A}_{1P} \\ \mathbf{A}_{21} & \mathbf{A}_{22} & \dots & \mathbf{A}_{2P} \\ \vdots & \vdots & \mathbf{A}_{kj} & \vdots \\ \mathbf{A}_{P1} & \mathbf{A}_{P2} & \dots & \mathbf{A}_{PP} \end{bmatrix} \begin{bmatrix} \bar{\mathbf{U}}_1 \\ \vdots \\ \bar{\mathbf{U}}_2 \\ \vdots \\ \bar{\mathbf{U}}_P \end{bmatrix} = \begin{bmatrix} \mathbf{F}_1 \\ \vdots \\ \mathbf{F}_j \\ \vdots \\ \mathbf{F}_P \end{bmatrix} \quad (18)$$

The submatrix  $\mathbf{A}_{kj}(\omega)$  is the product of the PC basis and system matrix and expressed as

$$\mathbf{A}_{kj}(\omega) = \sum_{i=0}^M \mathbb{E}[\mathbf{A}_i(\omega, \boldsymbol{\xi}) \Psi_k(\boldsymbol{\xi}) \Psi_j(\boldsymbol{\xi})] \quad (19)$$

Once the linear system equation of Eq. (18) is solved, the coefficients of the PCE basis are directly obtained.

The spectral projection method is one of the non-intrusive approaches, where the coefficients are obtained by utilizing orthogonality of the PC basis. Multiplying Eq. (11) by  $\Psi_j(\boldsymbol{\xi})$  and taking the expectation, the  $j$ th coefficients of the PC basis are computed as

$$\begin{aligned} \bar{\mathbf{U}}_j(\omega) &= \frac{1}{\mathbb{E}[\Psi_j^2(\boldsymbol{\xi})]} \mathbb{E}[\mathbf{U}(\omega, \boldsymbol{\xi}) \Psi_j(\boldsymbol{\xi})] \\ &= \frac{1}{\mathbb{E}[\Psi_j^2(\boldsymbol{\xi})]} \int \mathbf{U}(\omega, \boldsymbol{\xi}) \Psi_j(\boldsymbol{\xi}) f_{\boldsymbol{\xi}}(\boldsymbol{\xi}) d\boldsymbol{\xi} \end{aligned} \quad (20)$$

To carry out the integration of Eq. (20) the numerical quadrature is applied. The coefficients of the PC basis are obtained as

$$\bar{\mathbf{U}}_j(\omega) \simeq \frac{1}{\mathbb{E}[\Psi_j^2(\boldsymbol{\xi})]} \sum_{k=1}^{N_{\text{int}}} (\omega, \boldsymbol{\xi}^k) \Psi_j(\boldsymbol{\xi}^k) w_k \quad (21)$$

where  $w_k$ ,  $\boldsymbol{\xi}^k$ , and  $N_{\text{int}}$  are the weighting factor, integration point, and the number of integration points. At each integration point, one particular set of random parameters is determined. Based on these input values, the deterministic finite element solver is simulated to obtain the response.

### 3. Sensitivity based stabilization for spectral stochastic frequency response

#### 3.1 Rational function approximation using natural frequency sensitivity

Since the stochastic frequency response is highly sensitive to changes in random parameters near the natural frequencies, the conventional PCE (Eq. (11)) cannot predict the actual response (Jacquelin, Adhikari *et al.* 2014). Considering that the frequency response of a dynamic system is a rational function of modal characteristics, following Padé approximant is more appropriate to represent the solution (Jacquelin, Dessombz *et al.* 2017)

$$\mathbf{U}_k(\omega, \boldsymbol{\xi}) = \frac{\sum_{i=1}^{P_1} n_i(\omega) \Psi_i(\boldsymbol{\xi})}{\sum_{i=1}^{P_2} d_i(\omega) \Psi_i(\boldsymbol{\xi})} \quad (22)$$

where  $\mathbf{U}_k$ ,  $n_i$ , and  $d_i$ , are the scalar value of the response and the PC coefficients of the numerator and denominator;  $P_1$  and  $P_2$  are the numbers of PC basis for the numerator and denominator. Although Eq. (22) can approximate the non-regular characteristics near the natural frequencies, it is not easy to obtain the polynomial coefficients under multiple

random parameter cases (Chantramsi, Doostan *et al.* 2009). Moreover, since Padé approximants compute the response component-wisely, obtaining the stochastic response for vector-valued response may be cumbersome.

Therefore, to obtain the denominator more efficiently, an algorithm utilizing the natural frequency sensitivity is proposed. Before explaining the algorithm, damping is assumed to be proportional or lightly non-proportional. In this case, the  $j$ th modal damping coefficient can be computed using  $j$ th deterministic mode shape vector  $\boldsymbol{\Phi}_{oj}$  as  $c_j(\boldsymbol{\xi}) = \boldsymbol{\Phi}_{oj}^T \mathbf{C}(\boldsymbol{\xi}) \boldsymbol{\Phi}_{oj}$ . Based on the assumption, the following rational function is proposed to approximating the stochastic frequency response

$$\mathbf{U}(\omega, \boldsymbol{\xi}) = \frac{\sum_{j=1}^P \bar{\mathbf{U}}_j(\omega) \Psi_j(\boldsymbol{\xi})}{\prod_{j=1}^{N_e} [\omega_j^2(\boldsymbol{\xi}) - \omega^2 + i\omega c_j(\boldsymbol{\xi})]} \quad (23)$$

where  $N_e$  and  $\omega_j(\boldsymbol{\xi})$  are the number of considered natural frequencies within the range of interest and the  $j$ th random natural frequency. Referring to Eq. (23), the rational function is a combination of the conventional PCE method and the denominator of the random mode superposition method given by Eq. (24)

$$\mathbf{U}(\omega, \boldsymbol{\xi}) = \sum_{j=1}^{N_e} \frac{\boldsymbol{\Phi}_j(\boldsymbol{\xi}) \boldsymbol{\Phi}_j^T(\boldsymbol{\xi}) \mathbf{F}}{\omega_j^2(\boldsymbol{\xi}) - \omega^2 + i\omega c_j(\boldsymbol{\xi})} \quad (24)$$

where  $\boldsymbol{\Phi}_j(\boldsymbol{\xi})$  is the  $j$ th random mode shape vector. Since the random natural frequencies are still unknown in Eq. (23), first-order sensitivity (Fox and Kapoor 1968) is used to approximate random natural frequencies as follows:

$$\begin{aligned} \omega_j^2(\boldsymbol{\xi}) &\simeq \omega_{0j}^2 + \Delta\omega_j^2(\boldsymbol{\xi}) = \omega_{0j}^2 + \frac{\partial\omega_{0j}^2}{\partial\boldsymbol{\xi}} \boldsymbol{\xi} \\ \frac{\partial\omega_{0j}^2}{\partial\xi_k} &= \frac{1}{\boldsymbol{\Phi}_{0j}^T \mathbf{M}_0 \boldsymbol{\Phi}_{0j}} \boldsymbol{\Phi}_{0j}^T \left[ \frac{\partial\mathbf{K}}{\partial\xi_k} - \omega_{0j}^2 \frac{\partial\mathbf{M}}{\partial\xi_k} \right] \boldsymbol{\Phi}_{0j} \end{aligned} \quad (25)$$

where  $\omega_{0j}$ ,  $\Delta\omega_j(\boldsymbol{\xi})$  are the deterministic and stochastic part of the  $j$ th natural frequency. Similarly, the  $j$ th modal damping ratio can be linearized as  $c_j(\boldsymbol{\xi}) \simeq c_{0j} + \Delta c_j(\boldsymbol{\xi})$ , by using first-order Taylor expansion, where  $c_{0j}$ ,  $\Delta c_j(\boldsymbol{\xi})$  are the deterministic and linearized stochastic part of the  $j$ th modal damping coefficient. Once the deterministic and stochastic part of the natural frequencies and damping coefficients are computed, substituting these relations into Eq. (23) yields

$$\begin{aligned} \mathbf{U}(\omega, \boldsymbol{\xi}) &= \frac{\sum_{j=1}^P \bar{\mathbf{U}}_j(\omega) \Psi_j(\boldsymbol{\xi})}{\prod_{j=1}^{N_e} [\omega_{0j}^2 + \Delta\omega_j^2(\boldsymbol{\xi}) - \omega^2 + i\omega (c_{0j} + \Delta c_j(\boldsymbol{\xi}))]} \end{aligned} \quad (26)$$

The reason for utilizing the rational function in Eq. (26) rather than directly applying the random mode superposition in Eq. (23) is the complexity of the stochastic eigenvalue problem. In computing the stochastic eigensolution by applying the Galerkin method, nonlinear equations with size  $(N+1)P$  should be solved for one eigensolution. (Ghanem and Ghosh 2007); where  $N$  is the total DOF and  $P$  is the number of PC basis. Therefore, if the

number of considered modes increases, the computational cost will become prohibitive.

Although there is no unknown coefficients in the denominator of Eq. (26), one problem still remains is the polynomial order  $N_e$  for random variables. In order to reflect this behavior, the same PCE order  $N_e$  is required, and referring to Eq. (15), the number of the PC basis increases rapidly as the order increases. Therefore, to improve the computational efficiency, the unnecessary polynomials in the denominator must be removed. To tackle this issue, the Neumann series based selection strategy is proposed in this paper. At a given excitation frequency  $\omega$ , the  $j$ th denominator term of Eq. (26) can be expanded by utilizing Neumann series as follows:

$$\begin{aligned} & \frac{1}{\omega_{0j}^2 - \omega^2 + i\omega c_{0j}} \left( 1 + \frac{\Delta\omega_j^2(\xi) + i\omega\Delta c_j(\xi)}{\omega_{0j}^2 - \omega^2 + i\omega c_{0j}} \right)^{-1} \\ & = e_j \left( 1 + R_j(\xi) \right)^{-1} = e_j \sum_{k=0}^{\infty} \left( -R_j(\xi) \right)^k \end{aligned} \quad (27)$$

The condition for this series to converge is  $|R_j| < 1$ . The ratio  $R_j$  is stochastic and, to determine the convergence condition only depending on the excitation frequency, specific random parameters should be applied. In this paper, the maximum variation of random variables is considered to reflect the worst-case variability. For the unbounded case, the truncated random variables with a certain confidence interval can be applied. Applying this assumption to the convergence condition  $|R_j| < 1$ , the following relation is obtained

$$\left| \max_{\xi} |\Delta\omega_j^2(\xi) + i\omega\Delta c_j(\xi)| / \omega_{0j}^2 - \omega^2 + i\omega c_{0j} \right| < 1 \quad (28)$$

Based on the excitation frequency, the convergence condition of Eq. (28) can be checked. If the excitation frequency is far from the  $j$ th natural frequency, the denominator is much larger than the numerator such that Eq. (28) is easily satisfied. However, if the excitation frequency is close to the  $j$ th natural frequency, the denominator is close to zero and Eq. (28) is violated. Let  $\mathcal{A}$  be a set of natural frequencies which do not satisfy the convergence condition in Eq. (28). Utilizing this notation and Neumann series of Eq. (27), Eq. (26) becomes

$$\begin{aligned} & \mathbf{U}(\omega, \xi) \\ & = \frac{\left[ \sum_{j=1}^P \bar{\mathbf{U}}_j(\omega) \Psi_j(\xi) \right] \prod_{j \in \mathcal{A}^c} \left[ e_j \sum_{k=0}^{\infty} \left( -R_j(\xi) \right)^k \right]}{\prod_{j \in \mathcal{A}} \left[ \omega_{0j}^2 + \Delta\omega_j^2(\xi) - \omega^2 + i\omega \left( c_0 + \Delta c_j(\xi) \right) \right]} \end{aligned} \quad (29)$$

Referring to Eq. (29), the polynomial order of denominator  $N_e$  in Eq. (26) reduces to the cardinality of set  $|\mathcal{A}| = N_r$ . To further simplify Eq. (29), the PCE  $\sum_{j=1}^P \bar{\mathbf{V}}_j(\omega) \Psi_j(\xi)$  with the number of basis  $P$  is applied to approximate the numerator, and the following relation is obtained

$$\begin{aligned} & \mathbf{U}(\omega, \xi) \\ & \approx \frac{\sum_{j=1}^P \bar{\mathbf{V}}_j(\omega) \Psi_j(\xi)}{\prod_{j \in \mathcal{A}} \left[ \omega_{0j}^2 + \Delta\omega_j^2(\xi) - \omega^2 + i\omega \left( c_0 + \Delta c_j(\xi) \right) \right]} \\ & = \mathbf{N}(\omega, \xi) / D(\omega, \xi) \end{aligned} \quad (30)$$

where  $\bar{\mathbf{V}}_j$  is a coefficient vector of a PC basis.

It is worth noting that depending on the given excitation frequency  $\omega$ , the polynomial order of denominator in Eq. (30) is determined. If the excitation frequency is near the natural frequencies where Eq. (28) is violated, the rational function of Eq. (30) is maintained. However, when Eq. (28) is satisfied for all considered natural frequencies, in case that the excitation frequency is apart from natural frequencies, the  $N_r$  becomes zero and Eq. (30) is the same form as the conventional PCE. In this paper, such an approximation of the rational function is referred to as stabilized polynomial chaos expansion (SPCE), and its implementation to the spectral methods will be discussed in the next sub-section.

### 3.2 SPCE based spectral stochastic methods

Since the unknowns of SPCE coefficients are the same as the conventional PCE, it can be easily implemented into the conventional spectral stochastic methods as already discussed in section 2.3. For the Galerkin projection method, substituting Eq. (30) into Eq. (9), and multiplying the denominator  $D(\omega, \xi)$  yield the following relation

$$\sum_{i=0}^M \mathbf{A}_i(\omega, \xi) \sum_{j=1}^P \bar{\mathbf{V}}_j \Psi_j(\xi) = D(\omega, \xi) \mathbf{F}(\xi) \quad (31)$$

By forcing the residual of Eq. (31) to be orthogonal to each PC basis  $\Psi_k(\xi)$  for  $k=1, \dots, P$ , and take the expectation, the system of linear equations are obtained as follows:

$$\begin{aligned} & \sum_{i=0}^M \sum_{j=1}^P E[\Psi_k(\xi) \mathbf{A}_i(\omega, \xi) \Psi_j(\xi)] \bar{\mathbf{V}}_j \\ & = E[\Psi_k D(\omega, \xi) \mathbf{F}(\xi)] \end{aligned} \quad (32)$$

Comparing Eq. (17) and Eq. (32), the only difference between PCE and SPCE in the Galerkin projection method is the modification of the force vector on the right-hand side.

For the spectral projection method, the  $j$ th PC coefficients are obtained by multiplying Eq. (29) by  $\Psi_j(\xi) D(\omega, \xi)$  and taking the expectation operator as follows:

$$\bar{\mathbf{V}}_j(\omega) = \frac{1}{E[\Psi_j^2(\xi)]} E[\mathbf{U}(\omega, \xi) D(\omega, \xi) \Psi_j(\xi)] \quad (33)$$

By applying the numerical quadrature to Eq. (33), the  $j$ th PC coefficients are computed as

$$\bar{\mathbf{V}}_j(\omega) \approx \frac{1}{E[\Psi_j^2(\xi)]} \sum_{k=1}^{N_{\text{int}}} \mathbf{U}(\omega, \xi^k) D(\omega, \xi^k) \Psi_j(\xi^k) w_k \quad (34)$$

In the spectral projection method, the difference between PCE in Eq. (21) and SPCE in Eq. (34) is the presence of the denominator polynomials in the integral domain. Once the coefficients in the numerator are computed through the abovementioned procedures, the final rational function is obtained by dividing the denominator polynomials.

The proposed method has the following characteristics compared with the existing PC based methods for frequency response analysis: (1) it can effectively utilize the

information near the natural frequencies through the sensitivities; (2) it can be applied to both intrusive and non-intrusive methods of the existing spectral stochastic framework with slight modification; (3) there is no need to increase the order of polynomial chaos or discretize finer random space to reflect the non-smooth characteristics near the natural frequencies; (4) The proposed method can compute the polynomial coefficients for the vector-valued response directly; and (5) In terms of computational cost, the proposed algorithm requires additional computations for deterministic natural frequencies and their sensitivities within the frequency range of interests.

### 3.3 Calculation of response statistics

Once the coefficients for the spectral basis are computed, the response statistics can be easily obtained. The mean and variance of the  $k$ th DOF are defined as

$$\begin{aligned} \text{mean}(U_k(\omega)) &= \bar{U}_k(\omega) = E[U_k(\omega, \xi)] \\ \text{var}(U_k(\omega)) &= E\left[(U_k(\omega, \xi) - \bar{U}_k(\omega))^2\right] \end{aligned} \quad (35)$$

In calculating the response statistics, the difference between the conventional spectral and proposed method is that the orthogonal properties of the PCE cannot be utilized due to the form of the approximation function (Eq. (28)). Therefore, it is not possible to compute the response statistics directly, and an alternative approach should be employed. In this study, the Monte Carlo simulation (MCS) method is adopted to compute the response statistics. Since the original model problem is approximated by using the multivariate rational polynomials, the MCS under large samples are easily computed without computational burden. Given the sample sizes  $N_s$ , the response statistics in Eq. (35) are computed as

$$\begin{aligned} \bar{U}_k(\omega) &\simeq \frac{1}{N_s} \sum_{i=1}^{N_s} U_k(\omega, \xi^i) \\ \text{var}(U_k(\omega)) &\simeq \frac{1}{N_s - 1} \sum_{i=1}^{N_s} (U_k(\omega, \xi^i) - \bar{U}_k(\omega))^2 \end{aligned} \quad (36)$$

where  $U_k(\omega, \xi^i)$  is the  $k$ th DOF response of the  $i$ th sample.

## 4. Numerical examples

Prior to validating the proposed method through numerical studies, some implementation issues and the development environments are briefly discussed. All the algorithms mentioned above are developed with in-house code, written in the MATLAB 2017Ra. In performing some numerical operations, the following MATLAB commands are used: *eigs* for solving the eigenvalue problems, and *ksdensity* for estimating the probability density function (PDF). Finally, all numerical simulations are carried out on a personal desktop operating Windows 10 with Intel Core i7-7700K@4.2 GHz and 32 GB RAM.

### 4.1 Two degree-of-freedom (2-DOF) system

The first example is a two DOF system with stiffness variation, as shown in Fig. 1. The model is taken from

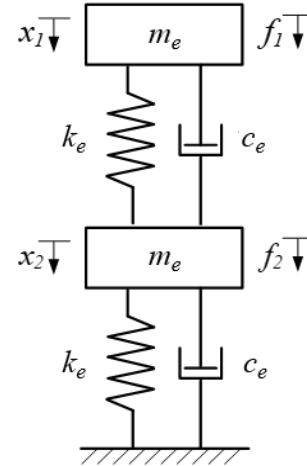


Fig. 1 2-DOF system with stochastic stiffness coefficient.

Table 1 System properties or the 2-DOF system

Properties	Value
$k_e$ (Nm <sup>-1</sup> )	15,000
$m_e$ (kg)	1
$c_e$ (Nm <sup>-1</sup> s <sup>-1</sup> )	1
$f_1$ (N)	1
$f_2$ (N)	0

Table 2 Deterministic modal characteristics of the 2-DOF system

Natural frequencies (Hz)	12.05	31.54
Damping ratio (%)	0.25	0.66

(Jacquelin, Adhikari *et al.* 2014). The model parameters and modal characteristics results are listed in Table 1 and Table 2. In this example, the stiffness  $k_e$  is assumed to be random and modeled as

$$k_e = \bar{k}_e(1 + 0.05\xi_k) \quad (37)$$

where  $\bar{k}_e$ ,  $\xi_k$  are mean stiffness and a standard normal random variable. Utilizing the Eq. (37), the random stiffness matrix  $\mathbf{K}_e$  is given by

$$\mathbf{K}_e = k_e \begin{bmatrix} 2 & -1 \\ -1 & 1 \end{bmatrix} \quad (38)$$

Before performing the stochastic analysis using PCE and SPCE, MCS with 10,000 samples are simulated to obtain the reference. The considered frequency range is 10–35 Hz with the interval  $\Delta f = 0.01$  Hz, and the quantity of interest point is  $x_1$ . Next, for polynomial degree  $p=2, 3$ , and 4, the Galerkin and spectral projection methods using PCE are applied. In carrying out the numerical integration in the spectral projection method, Gaussian-Hermite quadrature with  $N_{\text{int}}=5, 6$ , and 7 points are applied for each polynomial degree. The obtained mean and standard deviation results are presented in Fig. 2, where the abbreviation SP denotes the spectral projection method. It can be seen from the results that both two methods show spurious oscillation patterns around the two natural frequencies (12.05 and 31.54 Hz) for all considered polynomial degrees. However,

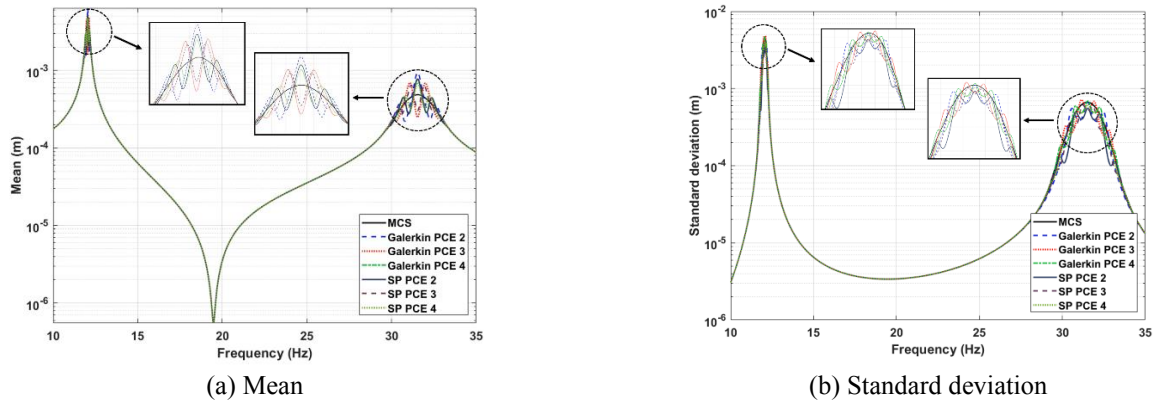


Fig. 2 Mean and standard deviation of the 2-DOF system. PCE with degree  $p=2, 3,$  and  $4$  are applied.

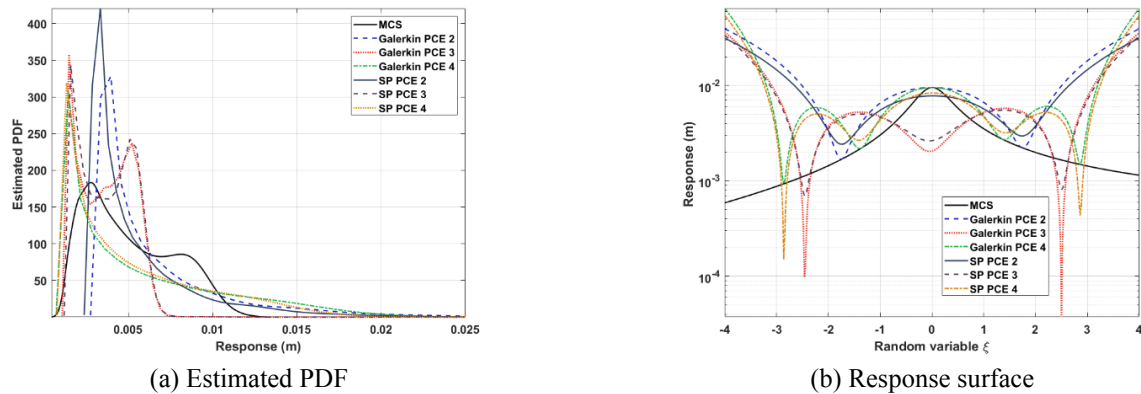


Fig. 3 Estimated PDF and response surface of the 2-DOF system at frequency 12.05 Hz. PCE with degree  $p=2, 3,$  and  $4$  are applied.

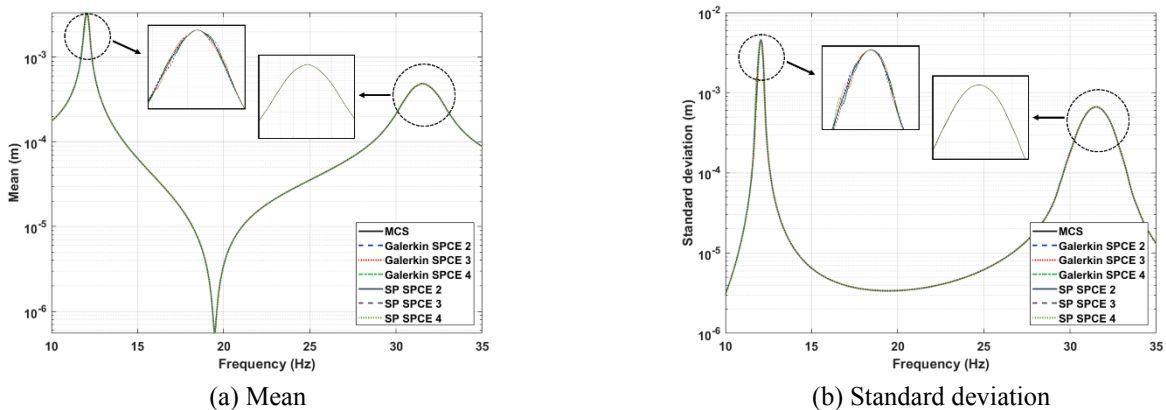
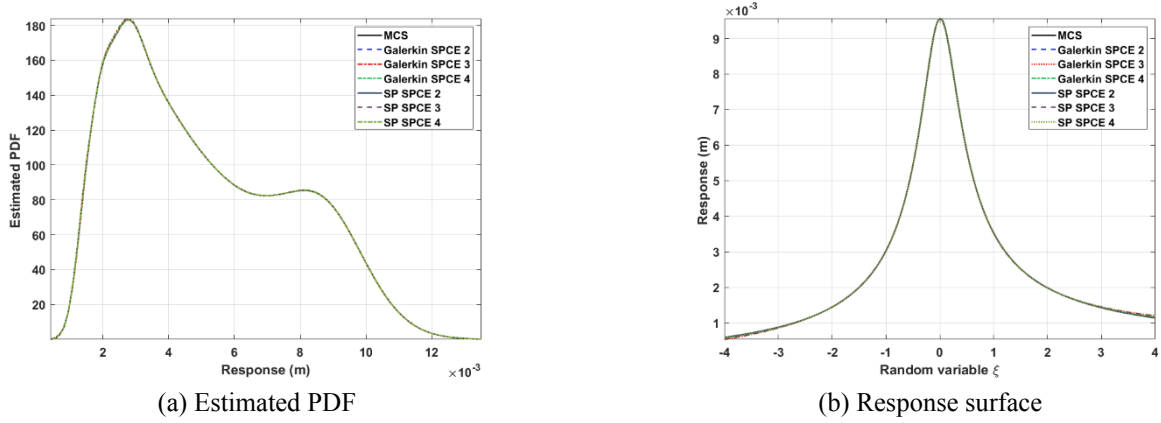


Fig. 4 Mean and standard deviation of the 2-DOF system. SPCE with degree  $p=2, 3,$  and  $4$  are applied.

if the excitation frequency is far from the natural frequencies, PCE can approximate the two statistical moments well. To further investigate the instability near the natural frequencies, the PDF and responses to the random variable are computed. The considered frequency is 12.05 Hz, which is the first undamped deterministic natural frequency, and the obtained results are given in Fig. 3. Since stochastic frequency response near the natural frequencies exhibits non-regular solution characteristics, approximating the response utilizing the polynomials gives erroneous results. Increasing the PCE order does not guarantee the accuracy and a wrong approximated model leads to inaccurate statistical properties, as shown in Fig. 2.

The proposed SPCE for the Galerkin and spectral projection methods are applied, and the two statistical moment results are presented in Fig. 4. The same number of quadrature used in PCE is applied. The results indicate that both two methods can stabilize suspicious oscillations near the natural frequencies and work well for all considered polynomial orders. This implies that a simple denominator in Eq. (29) can reflect the key solution characteristics near the natural frequencies. If excitation frequency is far from the natural frequencies, the results are the same as the PCE since there is no need to stabilize the response. The estimated PDF and response to the random variable at



(a) Estimated PDF

(b) Response surface

Fig. 5 Estimated PDF and response surface of the 2-DOF system at frequency 12.05 Hz. SPCE with degree  $p=2, 3,$  and  $4$  are applied.

Table 3 Mean and standard deviation error of the 2-DOF system. PCE and SPCE with polynomial degree  $p=2, 3,$  and  $4$  are considered.

PCE order	$\mathcal{E}_{\text{mean}}^{\text{PCE-G}}$	$\mathcal{E}_{\text{mean}}^{\text{PCE-SP}}$	$\mathcal{E}_{\text{mean}}^{\text{SPCE-G}}$	$\mathcal{E}_{\text{mean}}^{\text{SPCE-SP}}$	$\mathcal{E}_{\text{std}}^{\text{PCE-G}}$	$\mathcal{E}_{\text{std}}^{\text{PCE-SP}}$	$\mathcal{E}_{\text{std}}^{\text{SPCE-G}}$	$\mathcal{E}_{\text{std}}^{\text{SPCE-SP}}$
2	4.90E-1	3.38E-1	3.58E-2	2.03E-2	2.50E-1	2.72E-1	5.90E-2	3.48E-2
3	4.07E-1	2.96E-1	3.24E-2	2.06E-2	1.85E-1	2.05E-1	6.15E-2	3.71E-2
4	3.38E-1	2.51E-1	3.03E-2	2.14E-2	1.57E-1	1.66E-1	4.86E-2	3.81E-2

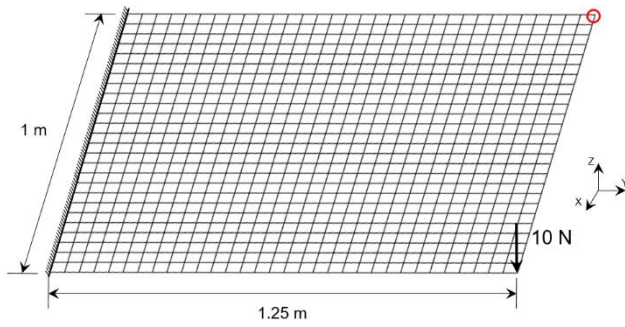


Fig. 6 Configuration of the rectangular panel. A point load is applied at the corner.

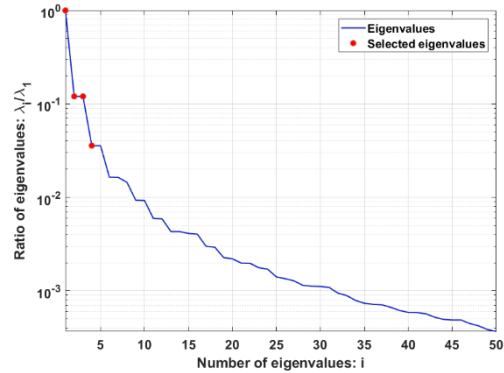


Fig. 7 The eigenvalue ratio results of the covariance function in the rectangular panel.

frequency 12.05 Hz are computed, and the results are given in Fig. 5. From the obtained results, it is apparent that SPCE can approximate the response within the random variable interval and it leads to an accurate estimation of statistical moments. To evaluate the performance, the mean and standard deviation errors are computed. In evaluating the error, the following error norm is applied and will be used in all the next examples

$$\mathcal{E}_s^m = \frac{\sqrt{\sum_{i=1}^{n_{\text{req}}} [\mathbf{u}_s^m(f_i) - \mathbf{u}_s^{\text{MCS}}(f_i)]^2}}{\sqrt{\sum_{i=1}^{n_{\text{req}}} [\mathbf{u}_s^{\text{MCS}}(f_i)]^2}} \quad (39)$$

where superscript  $s$ , subscript  $m$ , and  $n_{\text{req}}$  are the statistical moment, spectral method, the number of excitation frequency, respectively. The error results for PCE and SPCE methods are listed in Table 3, where the words G and SP after PCE- and SPCE- denote the Galerkin and spectral projection methods. A comparison of the error between PCE

and SPCE confirms that both errors in SPCE are reduced for all considered polynomial order.

#### 4.2 Rectangular panel

The second example is a rectangular panel, as illustrated in Fig. 6. A total of 891 nodes and 832 elements are applied to discretize the geometry using the quadrilateral elements. The model parameters are as follows: deterministic Young's modulus  $E_0=7 \times 10^7$  N/m<sup>2</sup>, Poisson ratio  $\nu=0.33$ , density  $\rho=2700$  kg/m<sup>3</sup>, and thickness  $t=5$  mm. In this example, Young's modulus  $E$  is assumed to be a Gaussian random field and represented using the truncated KL expansion as

$$E = E_0 \left( 1 + \sum_{i=1}^M \sqrt{\gamma_i} g_i(\mathbf{x}) \xi_i \right) \quad (40)$$

To obtain the eigensolution of the KL expansion problem in Eq. (3), following exponential covariance function is considered

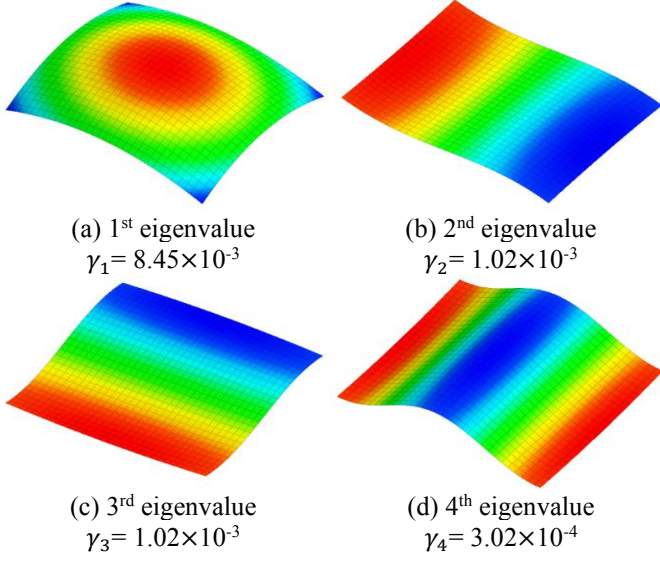


Fig. 8 First four eigensolutions of the covariance function in the rectangular panel

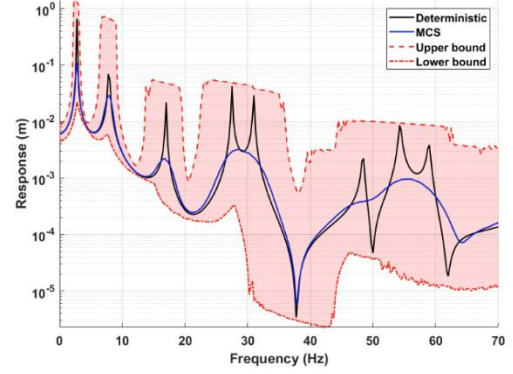
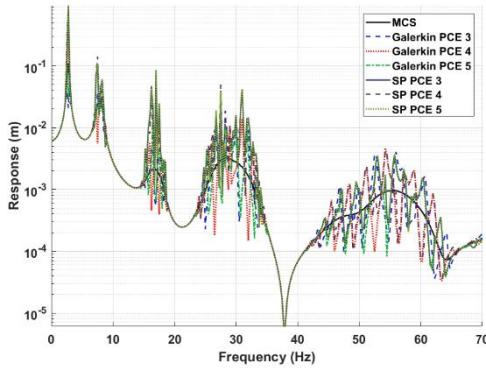


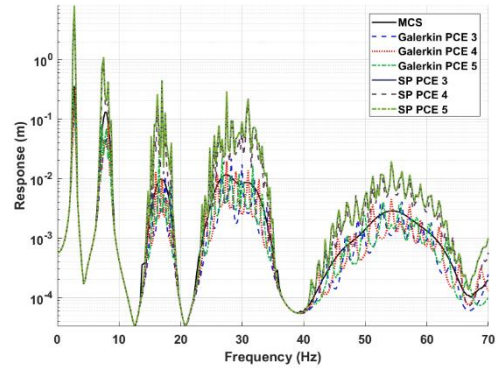
Fig. 9 Deterministic and MCS response of the rectangular panel. 15,000 samples are applied

Table 4 Deterministic modal characteristics of the rectangular panel

Natural frequencies (Hz)	2.73	7.86	16.93	27.44	30.93	48.32	54.25	58.82
Damping ratio (%)	0.30	0.15	0.15	0.20	0.22	0.32	0.35	0.38



(a) Mean



(b) Standard deviation

Fig. 10 Mean and standard deviation of the rectangular panel. PCE degree  $p=3, 4,$  and  $5$  are applied

$$C_E(\mathbf{x}_1, \mathbf{x}_2) = \sigma_E^2 \exp(-|x_1 - x_2|/l_x - |y_1 - y_2|/l_y) \quad (41)$$

where  $\sigma_E$ ,  $l_x$  and  $l_y$  are the standard deviation and the correlation length of  $x$  and  $y$ , respectively. Based on the discretized geometry and the parameters  $\sigma_E=0.1$ ,  $l_x=2$ , and  $l_y=1.6$ , the eigenvalue problem of the random field in Eq. (3) is conducted. The ratio of eigenvalues and the first four eigensolutions results are presented in Fig. 7 and Fig. 8. When applying 90% cut-off criterion for the random field discretization, four eigensolutions are required to simulate the given random field.

After obtaining the eigensolutions of the random field, the element stiffness matrix is computed as

$$\mathbf{K}^e = \mathbf{K}_0^e + \sum_{i=1}^4 \mathbf{K}_i^e \quad (42)$$

$$\mathbf{K}_0^e = \int \bar{\mathbf{B}}^T \mathbf{D}_0 \bar{\mathbf{B}} dV_e, \quad \mathbf{K}_i^e = \sqrt{\gamma_i} \int \mathbf{g}_i \bar{\mathbf{B}}^T \mathbf{D}_0 \bar{\mathbf{B}} dV_e$$

where  $\mathbf{K}_0^e$ ,  $\mathbf{K}_i^e$ ,  $\mathbf{D}_0$  and  $\bar{\mathbf{B}}$  are the deterministic and stochastic element stiffness matrix, constitutive, and strain-displacement matrix, respectively. In formulating the plate element, the assumed natural strain (ANS) method (Bathe and Dvorkin 1985) is applied to alleviate the transverse shear locking. Since the same meshes are used in random fields and structure problems, the stochastic stiffness matrix in Eq. (42) is directly computed by utilizing the nodal results of the eigenvector  $\mathbf{g}_i$ . In the end corner of the structure, a harmonic load 10 N is applied, and the end edge of the  $x$ -axis is subjected to a fixed boundary condition. The damping is modeled as proportional damping  $\mathbf{C} = \alpha \mathbf{M}_0 + \beta \mathbf{K}_0$  with the parameter  $\alpha = 10^{-1}$ ,  $\beta = 2 \cdot 10^{-5}$ . The frequency range under consideration is 0-70 Hz with the interval  $\Delta f = 0.25$  Hz. Within this frequency range, eight natural frequencies are included. Deterministic natural frequencies and modal damping ratio results are listed in Table 4.

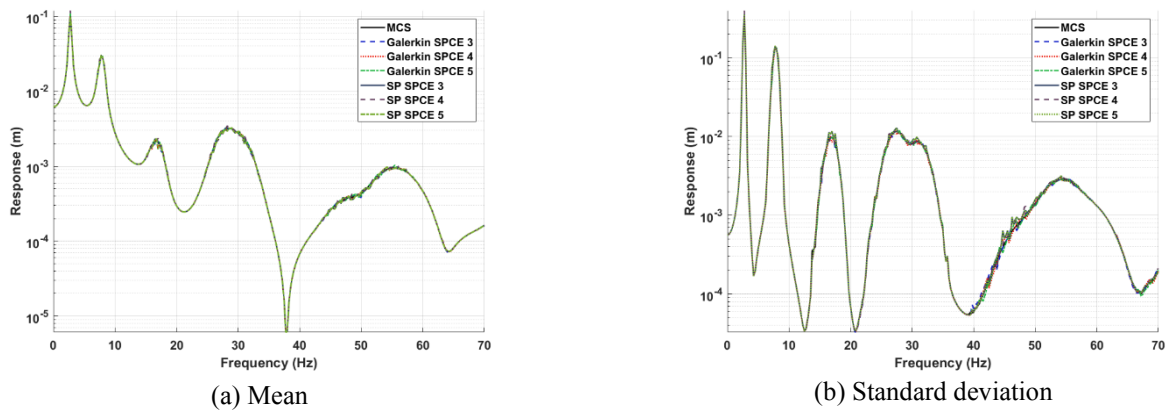


Fig. 11 Mean and standard deviation of the rectangular panel. SPCE with degree  $p=3, 4,$  and  $5$  are applied.

Table 5 Mean and standard deviation error of the rectangular panel. PCE and SPCE with polynomial degree  $p=3, 4,$  and  $5$  are considered

PCE order	$\mathcal{E}_{\text{mean}}^{\text{PCE-G}}$	$\mathcal{E}_{\text{mean}}^{\text{PCE-SP}}$	$\mathcal{E}_{\text{mean}}^{\text{SPCE-G}}$	$\mathcal{E}_{\text{mean}}^{\text{SPCE-SP}}$	$\mathcal{E}_{\text{std}}^{\text{PCE-G}}$	$\mathcal{E}_{\text{std}}^{\text{PCE-SP}}$	$\mathcal{E}_{\text{std}}^{\text{SPCE-G}}$	$\mathcal{E}_{\text{std}}^{\text{SPCE-SP}}$
3	8.39E-1	6.37E+0	1.40E-2	4.44E-2	7.25E-1	6.05E+0	1.73E-2	4.22E-2
4	1.91E+0	6.26E+0	2.60E-2	6.46E-2	4.20E-1	1.22E+1	3.02E-2	9.60E-2
5	1.03E+0	6.08E+0	2.04E-2	7.70E-2	7.37E-1	1.71E+1	2.87E-2	5.63E-2

In simulating the stochastic frequency response analysis, the MCS with 15,000 samples are applied to obtain the reference results. The quantity of interest is transverse displacement and the node position is indicated by the circle in Fig. 6. The deterministic and the MCS result with upper and lower bound are given in Fig. 9. When computing the deterministic results for 15,000 samples, about 800 seconds are required for each frequency. In this example, within the frequency range 25-35 Hz and 45-65 Hz, two and three deterministic natural frequencies are adjacent, respectively. Since the maximum peak response at the natural frequencies changes due to the random parameter variation, the min/max responses are widely distributed near the natural frequencies, and the mean results exhibit a smooth response compared to the deterministic response.

Next, the PCE using the Galerkin and spectral projection methods with polynomial order  $p=3, 4,$  and  $5$  are applied. Gaussian-Hermite quadrature with  $p+1$  for each random variable is considered in applying the spectral projection method. The mean and standard deviation results for PCE are presented in Fig. 10. Comparing the results of the MCS and PCE, it can be seen that except for the anti-resonant region, the obtained results are inaccurate within the given frequency ranges. Since deterministic natural frequencies are adjacent to each other, as shown in Fig. 9, the spurious oscillations corresponding to each natural frequency are superimposed. This implies that if the system has adjacent natural frequencies, the PCE results are deteriorated and can only be applied to a specific frequency range, which is sufficiently far from the natural frequencies.

The SPCE for the Galerkin and spectral projection methods are applied, and the two statistical moment results are presented in Fig. 11. The results indicate the statistical moments are well estimated over the entire frequency

range, even if natural frequencies are adjacent to each other. The slight error in the standard deviation is mainly due to the approximation of the stochastic natural frequencies via first-order sensitivities. However, although this slight error, both the Galerkin and spectral projection methods show performance improvement even with a low polynomial degree. This implies that denominator polynomials utilizing the sensitivity can play a crucial role in reflecting the uncertain dynamics near the natural frequencies. The mean and standard deviation error for the PCE and SPCE are listed in Table 5. By comparing the PCE and SPCE, the errors for SPCE are significantly reduced, and by comparing the Galerkin with the spectral projection methods, the Galerkin method shows better performance for all considered polynomial orders. Finally, at the frequencies,  $f=28$  and  $49$  Hz, which are near the 4<sup>th</sup> and 6<sup>th</sup> natural frequencies, the estimated PDF using the PCE and SPCE are given in Fig. 12. The obtained results indicate that although the PCE cannot capture the characteristics of the MCS, the SPCE reflects the overall solution behavior.

### 4.3 Simplified wing blade

The third example is a wing blade, as shown in Fig. 13. A total of 4,194 nodes and 3,810 elements are applied to discretize the geometry using low order triangular and quadrilateral elements. The model parameters used in this example are as follows: deterministic Young's modulus  $E_0=7.3 \times 10^7$  N/m<sup>2</sup>, Poisson ratio  $\nu=0.33$ , density  $\rho=2800$  kg/m<sup>3</sup>, and thickness  $t=2.54$  mm. In this example, Young's modulus  $E$  is assumed to be a Gaussian random field as

$$C_E(\mathbf{x}_1, \mathbf{x}_2) = \sigma_E^2 \exp(-|x_1 - x_2|/l_x - |y_1 - y_2|/l_y - |z_1 - z_2|/l_z) \quad (43)$$

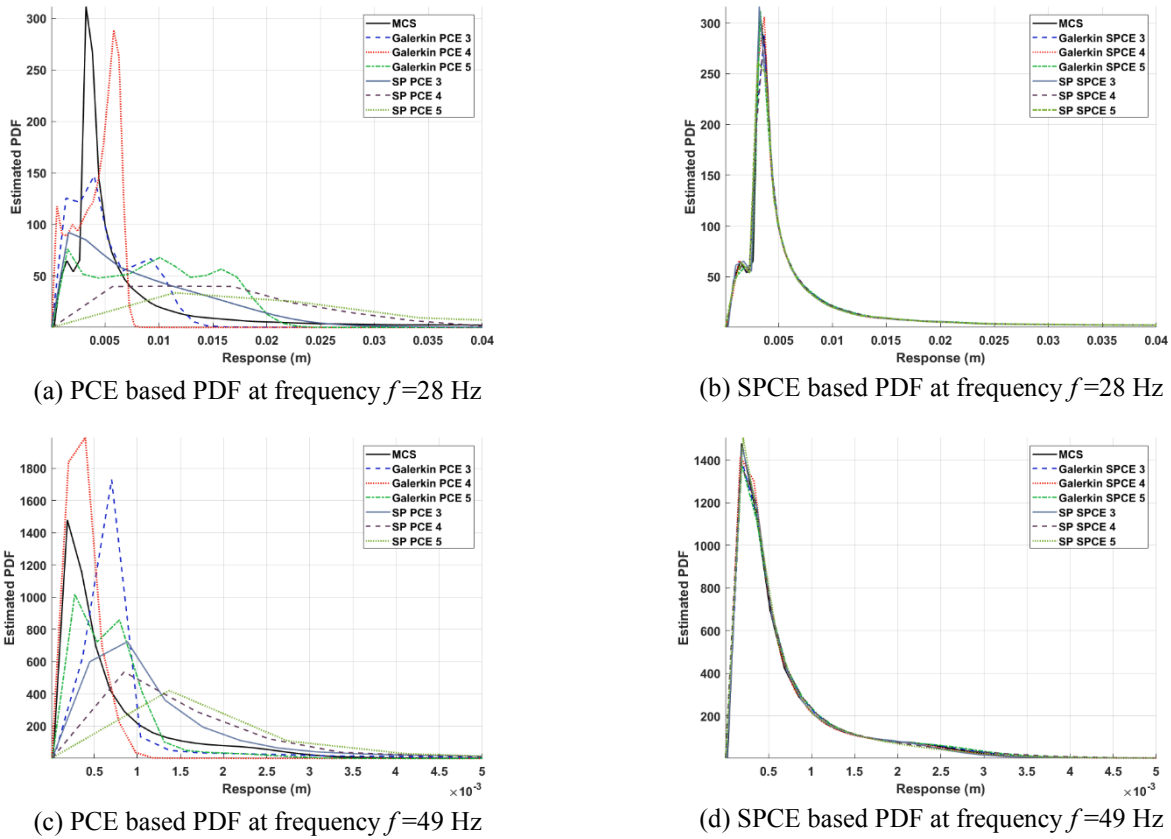


Fig. 12 Estimated PDF near the natural frequencies in the rectangular panel. PCE and SPCE with degree  $p=3, 4,$  and  $5$  are applied

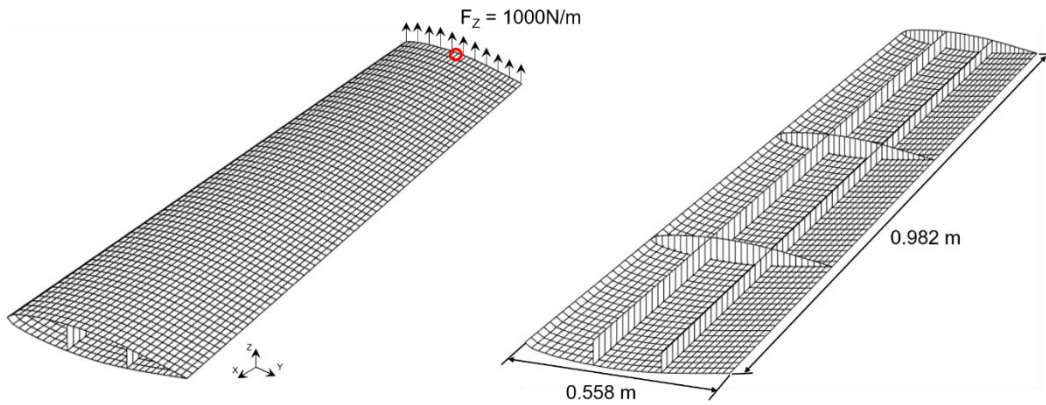


Fig. 13 Model of the simplified wing blade. A line load is applied at the end

The first four eigensolutions and ratio of the eigenvalue results are presented in Fig. 14 and Fig. 16. In this example, four eigensolutions of the covariance function are considered to simulate the given random field when applying a 90% truncation criterion. The stochastic stiffness matrix of the shell element is computed by combining the membrane stiffness and plate stiffness in Eq. (40).

Although the total DOF of the given structural system is 21,960, which is not quite large for the deterministic problem, the computational cost can be a burden for stochastic frequency response analysis. To avoid this issue, the model is reduced by the deterministic eigenvector as

proposed in (Pascual and Adhikari 2012). The 500 deterministic modes are considered, and the first four natural frequencies and mode shape vectors are given in Fig. 15. In the end part of the structure, a harmonic line load 10,000 N/m is applied, and the opposite end is subjected to a fixed boundary condition. The damping is modeled as proportional damping  $\mathbf{C} = \alpha \mathbf{M}_0 + \beta \mathbf{K}_0$ , where  $\alpha = 10^{-1}$ ,  $\beta = 10^{-5}$  are applied. The quantity of interest is displacement and the position is indicated by the circle in Fig. 13. The considered frequency range is 0-150 Hz, and an interval is  $\Delta f = 0.5$  Hz. Within the frequency range under consideration, the first three natural frequencies are

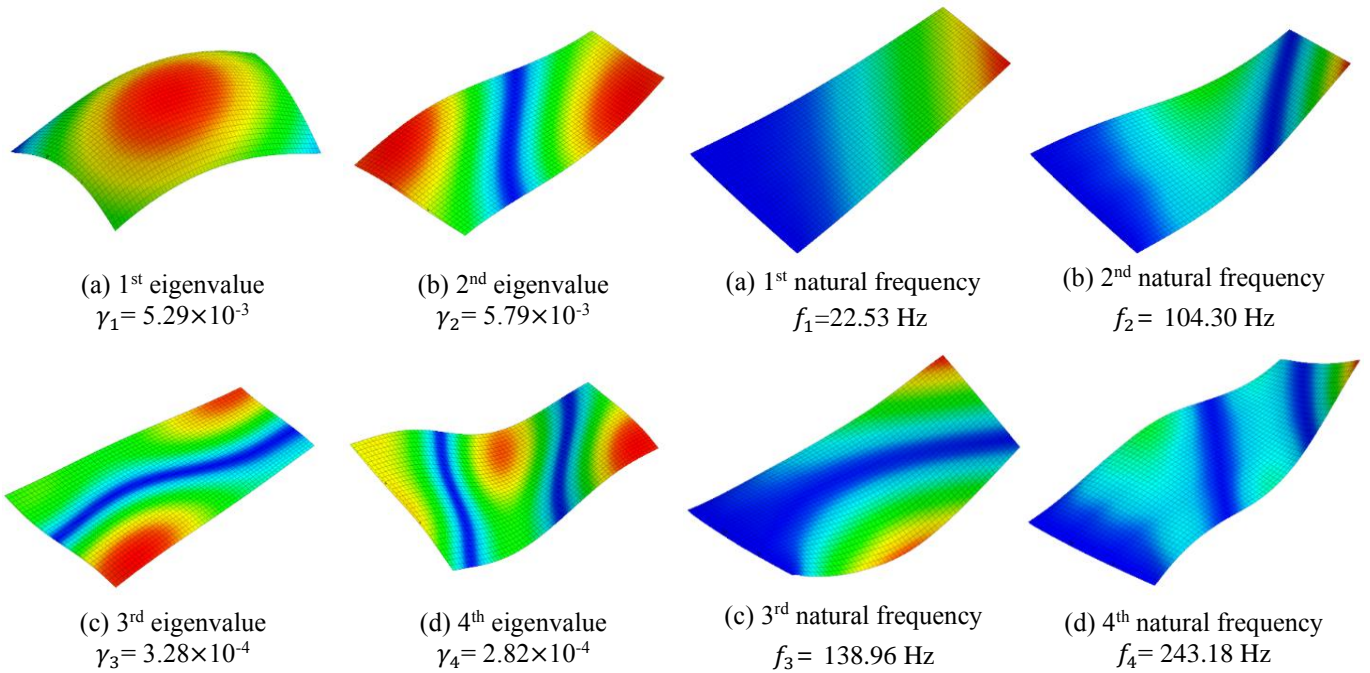


Fig. 14 First four eigensolutions of the covariance function in the wing blade

Fig. 15 First four natural frequencies and mode shape results of the wing blade

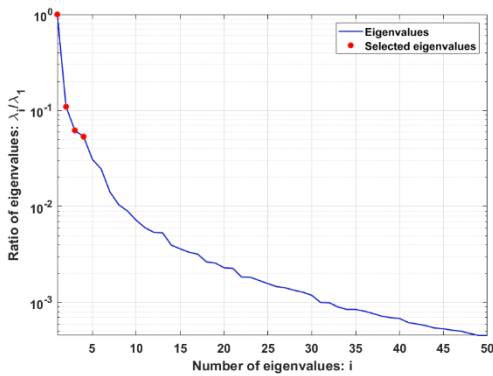


Fig. 16 The eigenvalue ratio results of the covariance function in the wing blade

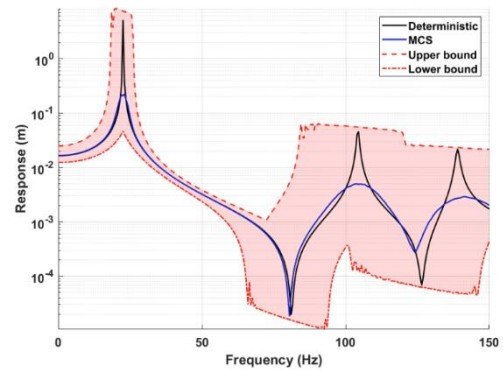
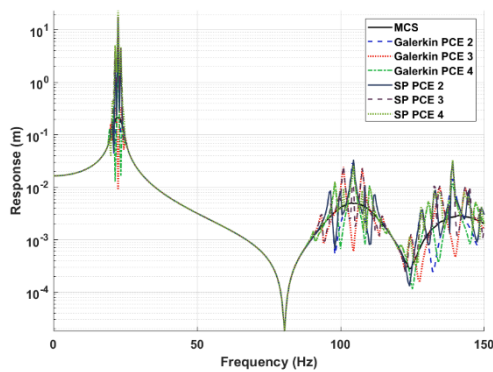
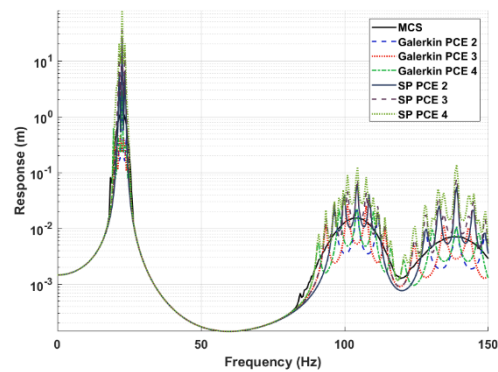


Fig. 17 Deterministic and MCS response of the wing blade. 15,000 samples are applied



(a) Mean



(b) Standard deviation

Fig. 18 Mean and standard deviation of the wing blade. PCE degree  $p=2, 3,$  and  $4$  are applied

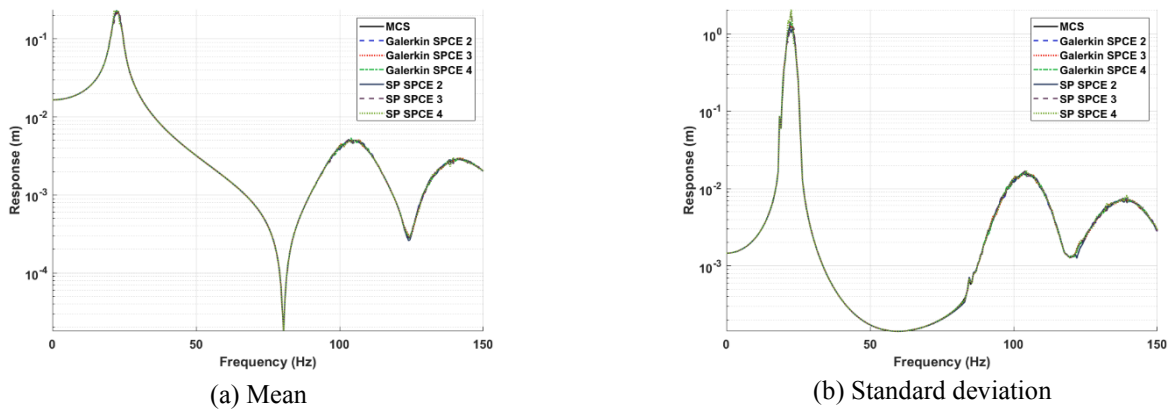


Fig. 19 Mean and standard deviation of the wing blade. SPCE degree  $p=2, 3,$  and  $4$  are applied

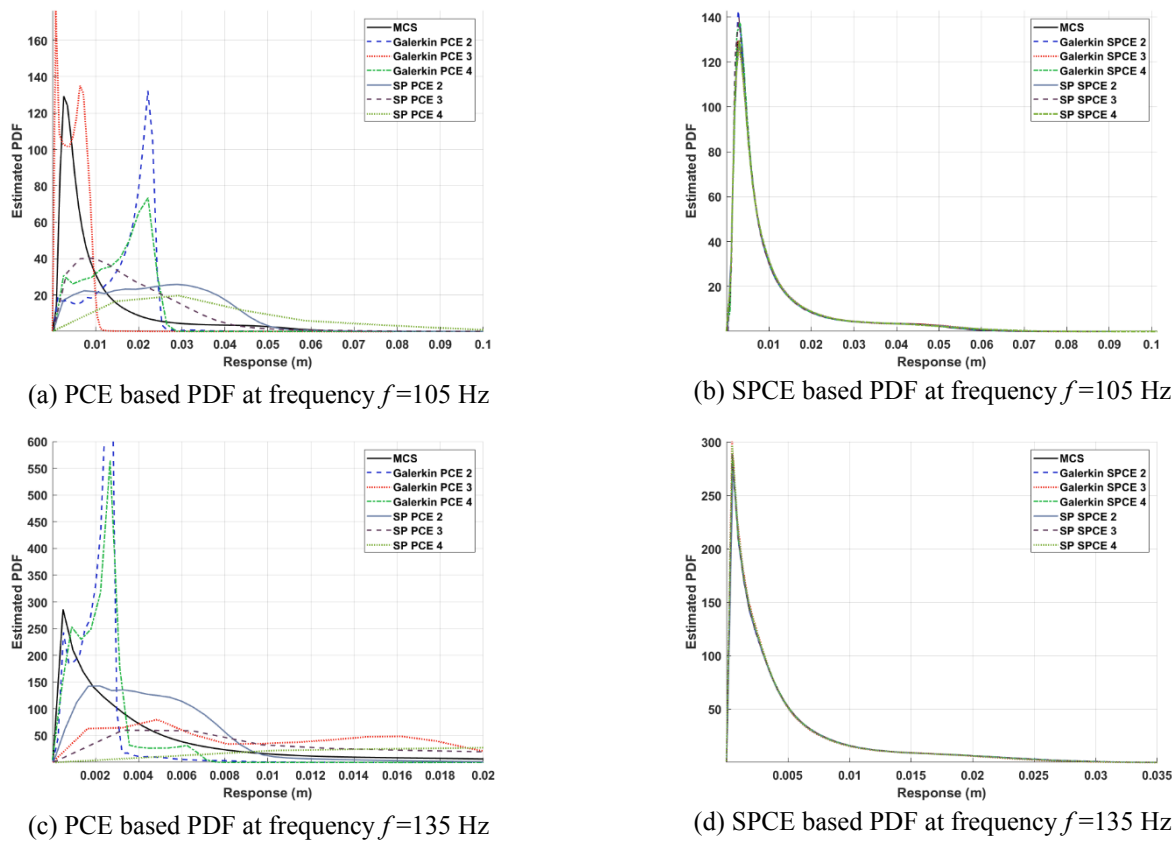


Fig. 20 Estimated PDF near the natural frequencies in the wing blade. PCE and SPCE with degree  $p=2, 3,$  and  $4$  are applied

included, and each corresponding modal damping ratio is 0.10, 0.33, and 0.44 %, respectively.

In simulating the stochastic frequency analysis, the MCS using 15,000 samples are applied to obtain the reference results. The stochastic and deterministic results are presented in Fig. 17. The results indicate that within the frequency range of 100-150 Hz, two natural frequencies are close to each other. Since natural frequencies due to the random parameter variation significantly affect the response variability, the min/max responses are distributed, as studied in the previous example.

Next, the PCE and SPCE utilizing the Galerkin and the spectral methods are applied, and the two statistical moment

results are represented in Fig. 18 and Fig. 19, respectively. It can be seen from the results that although the PCE methods can estimate the statistical response within the frequency range of 30-85 Hz, which are far from the first and second natural frequencies, the accuracy is degraded near the natural frequencies. However, SPCE can well estimate the stochastic frequency response over the entire frequency range for all considered polynomial degrees.

Finally, near the two natural frequencies  $f=105, 135$  Hz, the PDF applying the PCE and SPCE are estimated, and their results are given in Fig. 20. These excitation frequencies are close to the second and third natural frequencies of the deterministic system. The obtained

Table 6 Mean and standard deviation error of the wing blade. PCE and SPCE with polynomial degree  $p=2, 3$ , and 4 are considered

PCE order	$\epsilon_{\text{mean}}^{\text{PCE-G}}$	$\epsilon_{\text{mean}}^{\text{PCE-SP}}$	$\epsilon_{\text{mean}}^{\text{SPCE-G}}$	$\epsilon_{\text{mean}}^{\text{SPCE-G}}$	$\epsilon_{\text{std}}^{\text{PCE-G}}$	$\epsilon_{\text{std}}^{\text{PCE-SP}}$	$\epsilon_{\text{std}}^{\text{SPCE-G}}$	$\epsilon_{\text{std}}^{\text{SPCE-SP}}$
2	6.14E+0	2.60E+1	1.03E-1	1.37E-1	8.99E-1	8.98E+0	8.50E-2	7.90E-2
3	1.21E+0	3.47E+1	2.62E-2	2.16E-1	7.08E-1	1.38E+1	3.70E-2	2.78E-1
4	4.89E+0	4.19E+1	9.08E-2	3.38E-1	9.12E-1	2.99E+1	7.58E-2	3.56E-1

results indicate that none of the estimated PDF applying the PCE matches the MCS results. Especially for the spectral stochastic method, the estimated PDF results are widespread and give completely erroneous results. However the SPCE methods using the Galerkin and spectral stochastic techniques capture the overall response characteristics of the reference result. The mean and standard deviation error for PCE and SPCE are given in Table 6. All obtained results demonstrate that the proposed SPCE can improve the accuracy even with low order polynomials.

## 5. Conclusions

In this study, a natural frequency sensitivity-based stabilization framework for SSFEM is proposed to compute the stochastic frequency response. The approximated solution form is a rational function, where the numerator term is the conventional PCE method, and the denominator is the proposed sensitivity of natural frequencies. Since the proposed approximation can increase the PCE order, active denominators are remained by examining the given excitation frequency. The proposed algorithm is applied to two commonly used spectral stochastic methods with slight modification.

To validate the performance, three examples of stochastic frequency response are considered. The first example is the 2-DOF spring-mass system. The second and third examples are the rectangular panel and simplified wing blade models. The obtained results are in good agreement with the direct MCS simulation in the entire considered frequency range, although the conventional PCE cannot predict the actual response near the natural frequencies. This is attributed to the denominator term, which can reflect the key solution characteristics near the natural frequencies. The proposed method is promising for both accuracy and numerical efficiency and is expected to be applied to other stochastic frequency response problems.

In this paper, only material uncertainties are considered, and the damping model is assumed to be a proportional case. Therefore, further research on various types of uncertainties and non-proportional or non-viscous damping is needed to generalize the proposed framework.

## Acknowledgments

This work was supported by ‘‘Human Resources Program in Energy Technology’’ of the Korea Institute of

Energy Technology Evaluation and Planning (KETEP), granted financial resource from the Ministry of Trade, Industry & Energy, Republic of Korea. (No.20184030202000).

## References

- Adhikari, S. (2011), ‘‘Doubly spectral stochastic finite-element method for linear structural dynamics’’, *J. Aerosp. Eng.*, **24**(3), 264-276. [https://doi.org/10.1061/\(ASCE\)AS.1943-5525.0000070](https://doi.org/10.1061/(ASCE)AS.1943-5525.0000070)
- Adhikari, S. and Pascual, B. (2016), ‘‘The ‘damping effect’ in the dynamic response of stochastic oscillators’’, *Probabilistic Eng. Mech.*, **44**, 2-17. <https://doi.org/10.1016/j.probengmech.2015.09.017>
- Bathe, K.J. and Dvorkin, E.N. (1985), ‘‘A four-node plate bending element based on Mindlin/Reissner plate theory and a mixed interpolation’’, *J. Numerical Methods Eng.*, **21**(2), 367-383. <https://doi.org/10.1002/nme.1620210213>
- Berveiller, M., Sudret, B. and Lemaire, M. (2006), ‘‘Stochastic finite element: a non intrusive approach by regression’’, *European Journal of Computational Mechanics/Revue Européenne de Mécanique Numérique*, **15**(1-3), 81-92. <https://doi.org/10.3166/remn.15.81-92>
- Blatman, G. and Sudret, B. (2011), ‘‘Adaptive sparse polynomial chaos expansion based on least angle regression’’, *J. Comput. Phys.*, **230**(6), 2345-2367. <https://doi.org/10.1016/j.jcp.2010.12.021>
- Chantrasmı, T., Doostan, A. and Iaccarino, G. (2009), ‘‘Padé-Legendre approximants for uncertainty analysis with discontinuous response surfaces’’, *J. Comput. Phys.*, **228**(19), 7159-7180. <https://doi.org/10.1016/j.jcp.2009.06.024>
- Chevreuril, M. and Nouy, A. (2012), ‘‘Model order reduction based on proper generalized decomposition for the propagation of uncertainties in structural dynamics’’, *J. Numerical Methods Eng.*, **89**(2), 241-268. <https://doi.org/10.1002/nme.3249>
- Fox, R. and Kapoor, M. (1968), ‘‘Rates of change of eigenvalues and eigenvectors’’, *AIAA J.*, **6**(12), 2426-2429. <https://doi.org/10.2514/3.5008>
- Galal, O., El-Tahan, W., El-Tawil, M. and Mahmoud, A. (2008), ‘‘Spectral SFEM analysis of structures with stochastic parameters under stochastic excitation’’, *Struct. Eng. Mech.*, **28**(3), 281-294. <https://doi.org/10.12989/sem.2008.28.3.281>
- Ghanem, R. and Ghosh, D. (2007), ‘‘Efficient characterization of the random eigenvalue problem in a polynomial chaos decomposition’’, *J. Numerical Methods Eng.*, **72**(4), 486-504.
- Ghanem, R.G. and Spanos, P.D. (2003), *Stochastic Finite Elements: A Spectral Approach*, Courier Corporation, MA, USA.
- Hurtado, J. and Barbat, A.H. (1998), ‘‘Monte Carlo techniques in computational stochastic mechanics’’, *Arch. Comput. Methods Eng.*, **5**(1), 3. <https://doi.org/10.1007/BF02736747>
- Hussein, A., El-Tawil, M., El-Tahan, W. and Mahmoud, A. (2008), ‘‘Solution of randomly excited stochastic differential equations with stochastic operator using spectral stochastic finite element method (SSFEM)’’, *Struct. Eng. Mech.*, **28**(2), 129-152. <https://doi.org/10.12989/sem.2008.28.2.129>
- Jacquelin, E., Adhikari, S., Friswell, M. and Sinou, J.-J. (2016),

- “Role of roots of orthogonal polynomials in the dynamic response of stochastic systems”, *J. Eng. Mech.*, **142**(8), 06016004. [https://doi.org/10.1061/\(ASCE\)EM.1943-7889.0001102](https://doi.org/10.1061/(ASCE)EM.1943-7889.0001102)
- Jacquelin, E., Adhikari, S., Sinou, J.-J. and Friswell, M.I. (2014), “Polynomial chaos expansion and steady-state response of a class of random dynamical systems”, *J. Eng. Mech.*, **141**(4), 04014145. [https://doi.org/10.1061/\(ASCE\)EM.1943-7889.0000856](https://doi.org/10.1061/(ASCE)EM.1943-7889.0000856)
- Jacquelin, E., Adhikari, S., Sinou, J.J. and Friswell, M.I. (2015), “Polynomial chaos expansion in structural dynamics: Accelerating the convergence of the first two statistical moment sequences”, *J. Sound Vib.*, **356**, 144-154. <https://doi.org/10.1016/j.jsv.2015.06.039>
- Jacquelin, E., Dessombz, O., Sinou, J.J., Adhikari, S. and Friswell, M.I. (2017), “Polynomial chaos-based extended Padé expansion in structural dynamics”, *J. Numerical Methods Eng.*, **111**(12), 1170-1191. <https://doi.org/10.1002/nme.5497>
- Kleiber, M. and Hien, T.D. (1992), *The Stochastic Finite Element Method: Basic Perturbation Technique and Computer Implementation*, Wiley, New Jersey, USA.
- Kundu, A., Adhikari, S. and Friswell, M. (2014), “Stochastic finite elements of discretely parameterized random systems on domains with boundary uncertainty”, *J. Numerical Methods Eng.*, **100**(3), 183-221. <https://doi.org/10.1002/nme.4733>
- Nouy, A. (2007), “A generalized spectral decomposition technique to solve a class of linear stochastic partial differential equations”, *Comput. Methods Appl. Mech. Eng.*, **196**(45-48), 4521-4537. <https://doi.org/10.1016/j.cma.2007.05.016>.
- Pagnacco, E., Sarrouy, E., Sampaio, R. and de Cursi, E.S. (2017), “Pitfalls in the frequency response represented onto Polynomial Chaos for random SDOF mechanical systems”, *Applied Mathematical Modelling*, **52**, 626-647. <https://doi.org/10.1016/j.apm.2017.08.004>
- Papadrakakis, M. and Papadopoulos, V. (1996), “Robust and efficient methods for stochastic finite element analysis using Monte Carlo simulation”, *Comput. Methods Appl. Mech. Eng.*, **134**(3-4), 325-340. [https://doi.org/10.1016/0045-7825\(95\)00978-7](https://doi.org/10.1016/0045-7825(95)00978-7)
- Pascual, B. and Adhikari, S. (2012), “A reduced polynomial chaos expansion method for the stochastic finite element analysis”, *Sadhana*, **37**(3), 319-340. <https://doi.org/10.1007/s12046-012-0085-1>.
- Sakamoto, S. and Ghanem, R. (2002), “Simulation of multi-dimensional non-Gaussian non-stationary random fields”, *Probabilistic Eng. Mech.*, **17**(2), 167-176. [https://doi.org/10.1016/S0266-8920\(01\)00037-6](https://doi.org/10.1016/S0266-8920(01)00037-6).
- Sepahvand, K. (2016), “Spectral stochastic finite element vibration analysis of fiber-reinforced composites with random fiber orientation”, *Compos. Struct.*, **145**, 119-128. <https://doi.org/10.1016/j.compstruct.2016.02.069>.
- Sinou, J.J. and Jacquelin, E. (2015), “Influence of Polynomial Chaos expansion order on an uncertain asymmetric rotor system response”, *Mech. Syst. Signal Process.*, **50**, 718-731. <https://doi.org/10.1016/j.ymsp.2014.05.046>.
- Smith, R.C. (2013), *Uncertainty Quantification: Theory, Implementation, and Applications*, Siam, PH, USA.
- Stefanou, G. (2009), “The stochastic finite element method: past, present and future”, *Computer Methods Appl. Mech. Eng.*, **198**(9-12), 1031-1051. <https://doi.org/10.1016/j.cma.2008.11.007>
- Xiu, D. and Hesthaven, J.S. (2005), “High-order collocation methods for differential equations with random inputs”, *SIAM Journal on Scientific Computing*, **27**(3), 1118-1139. <https://doi.org/10.1137/040615201>
- Xiu, D. and Karniadakis, G.E. (2002), “The Wiener-Askey polynomial chaos for stochastic differential equations”, *SIAM J. Sci. Comput.*, **24**(2), 619-644. <https://doi.org/10.1137/S1064827501387826>
- Yamazaki, F., Shinozuka, M. and Dasgupta, G. (1988), “Neumann expansion for stochastic finite element analysis”, *J. Eng. Mech.*, **114**(8), 1335-1354 [https://doi.org/10.1061/\(ASCE\)0733-9399\(1988\)114:8\(1335\)](https://doi.org/10.1061/(ASCE)0733-9399(1988)114:8(1335))

PL